Development and Verification of Distributed Real-Time Hybrid Simulation Methods

Xin Li[1]; Ali I. Ozdagli[2]; Shirley J. Dyke, A.M.ASCE[3]; Xilin Lu[4]; and Richard Christenson, M.ASCE[5]

Abstract: Hybrid simulation combines numerical simulation and physical testing, and is thus considered to be an efficient alternative to traditional testing methodologies in the evaluation of global performance of large or complex structures. Real-time hybrid simulation (RTHS) is performed when it is important to fully capture rate-dependent behaviors in the physical substructure. Although the demand to test more complex systems grows, not every laboratory has the right combination of computational and equipment resources available to perform large-scale experiments. Distributed real-time hybrid simulation (dRTHS) facilitates testing that is to be conducted at multiple geographically distributed laboratories while utilizing the Internet to couple the substructures. One major challenge in dRTHS is to accommodate the unpredictable communication time delays between the various distributed sites that occur as a result of Internet congestion. Herein, a dRTHS framework is proposed where a modified Smith predictor is adopted to accommodate such communication delays. To examine and demonstrate the sensitivity of the proposed framework to communication delays and to modeling errors, parametric analytical case studies are presented. Additionally, the effectiveness of this dRTHS framework is verified through successful execution of multisite experiments. The results demonstrate that this framework provides a new option for researchers to evaluate the global response of structural systems in a distributed real-time environment. **DOI: 10.1061/(ASCE)CP.1943-5487.0000654.**

Author keywords: Distributed real-time hybrid simulation; Smith predictor; Magnetorheological damper.

Introduction

Buildings that are subjected to strong ground motions may experience catastrophic damage. It is essential to provide earthquake-resistant designs for new structures and to evaluate the safety of existing structures that reside in seismic regions to mitigate earthquake damage and extend the lifecycle of current civil infrastructure. Two main approaches have traditionally been used to examine the seismic performance of structural systems: performing a computational simulation, and conducting a physical experiment. The dynamic response of an untested complex structural system is often difficult to model and predict through pure computational simulation, and thus numerical models are frequently updated or improved with the information provided through experiments.

Several experimental methods are currently being used to study such dynamic response, including shake-table testing, quasi-static testing, and hybrid simulation methods. Hybrid simulation for mechanical systems originated in the 1970s (Takanashi et al. 1975). This approach integrated numerical computation and physical testing to represent an entire structure, and aimed to examine an untested physical specimen under quite realistic conditions. It was accepted as a cost- and time-effective alternative to traditional shake-table testing and quasi-static testing (Mahin et al. 1989; Magonette and Negro 1998; Nakashima 2001).

The potential of hybrid simulation has been further extended by exploiting the combined capacity across multiple geographically distributed laboratories, linking the experimental and numerical substructures through the Internet (Campbell and Stojadinovic 1998). Geographically distributed hybrid simulation allows researchers to conduct more complex experiments and simulations on structural systems at multiple equipment sites that could not be performed at a single site because of laboratory capacity limitations. Early examples of distributed hybrid simulation frameworks were between Japan and Korea using the Platform for Networked Structural Experiments (Watanabe et al. 2001) and in Taiwan (Tsai et al. 2003). In the United States, during 2000–2014, the National Science Foundation (NSF) provided financial resources to establish a shared infrastructure for earthquake engineering experimentation. This infrastructure consisted of 15 shared-use equipment sites located throughout the United States, and an associated cyber infrastructure connecting them through a grid-based middleware. Together, these were known as the George E. Brown Jr. Network for Earthquake Engineering Simulation (NEES). Under the NEES program, the multisite online simulation test (MOST) and mini-MOST experiments demonstrated the significant potential of distributed capabilities for hybrid simulation (Spencer et al. 2004). Highly advanced testing was enabled through broad researcher access to this shared-use infrastructure. For instance, Mosqueda et al. developed a continuous control method for performing hybrid simulation using distributed sites (2004); Shing et al. developed a fast hybrid test (FHT) system with a shared common RAM network using *OpenSees* for computational simulation (2004); Takahashi et al. designed a software framework for distributed experimental-computational simulation of structural systems (2006). Additionally, the multisite soil-structure-foundation interaction test (MISST) was performed by collaborating partners at the University of Illinois at Urbana-Champaign, Lehigh University, and Rensselaer Polytechnic

[1]Ph.D. Candidate, College of Civil Engineering, Tongji Univ., Shanghai 200092, China. E-mail: cindylixin1988@gmail.com

[2]Research Fellow, Lyles School of Civil Engineering, Purdue Univ., West Lafayette, IN 47906. E-mail: aozdagli@purdue.edu

[3]Professor, Dept. of Mechanical Engineering, Purdue Univ., West Lafayette, IN 47906. E-mail: sdyke@purdue.edu

[4]Professor, College of Civil Engineering, Tongji Univ., Shanghai 200092, China (corresponding author). E-mail: lxlst@tongji.edu.cn

[5]Associate Professor, Civil and Environment Engineering, Univ. of Connecticut, CT 06269. E-mail: rchriste@engr.uconn.edu

Note. This manuscript was submitted on October 20, 2015; approved on October 5, 2016; published online on February 23, 2017. Discussion period open until July 23, 2017; separate discussions must be submitted for individual papers. This paper is part of the ***Journal of Computing in Civil Engineering***, © ASCE, ISSN 0887-3801.

Institute to verify and extend the NEES hardware and middleware (Elnashai et al. 2008).

Hybrid simulation has traditionally been performed at an extended time scale. When it is necessary to capture rate-dependent dynamic behavior of critical physical substructures (e.g., dampers, friction devices, and base isolation), real-time hybrid simulation (RTHS) is needed (Gao et al. 2013; Friedman et al. 2014). In RTHS, the computations associated with each numerical integration time step during the combined numerical-physical experiment must be executed within the true clock time window, or in other words, at *real time* (Nakashima and Masaoka 1999; Diming et al. 1999). As such, the development of distributed RTHS (dRTHS) methods introduces numerous technical challenges, but also offers several opportunities.

One major challenge in the execution of successful dRTHS is in accommodating the unpredictable communication time delays occurring because of the fluctuations in Internet traffic (Maghareh et al. 2014a). Network delays within the United States can vary from tens to thousands of milliseconds and generally depend on the current condition of Internet traffic. These delays are significantly larger than the communication delays typically experienced between testing equipment within a single laboratory when conducting RTHS. However, no matter the source of delay, real-time execution cannot be reliably conducted without proper compensation for the actual delays present (Maghareh et al. 2014a; Ou et al. 2015).

Only a few studies to date have focused on the execution of dRTHS. Kim et al. proposed a dRTHS approach using a Smith predictor to overcome the effects of network delay. The effectiveness of this framework was demonstrated through a series of tests conducted at a rate of 500 Hz between the University of Connecticut (UConn) and the University of Illinois (Kim et al. 2012). Ojaghi et al. proposed a large time-step prediction algorithm to overcome both local actuation and distributed system delays (2014). The resulting approach was intended for applications with large integration time steps of up to 50 Hz. For examination of typical structural behaviors using RTHS, a sampling rate of 1,000 Hz has become common owing to the need for relatively high sampling rates needed to achieve good actuator tracking control (Maghareh et al. 2014b). The aforementioned platforms used in the past for dRTHS experiments have not achieved this rate.

This paper presents a framework to conduct geographically distributed RTHS. A modified Smith predictor is introduced to accommodate network communication delays, and thus enable dRTHS. The sensitivity of the framework to time delays and modeling errors is first examined through parametric studies of both linear and nonlinear systems considering (1) a linear spring, and (2) a nonlinear magnetorheological (MR) damper. Next, to verify the performance of the dRTHS framework, a set of experiments is discussed involving a two-story building model with one MR damper between the first floor of the structure and the ground. Both, a single-site (at Purdue University) and multisite RTHS (also involving the University of Connecticut) are conducted. Robust integrated actuator control (RIAC) is used to enforce boundary conditions and achieve proper actuator control in RTHS (Ou et al. 2015). To execute dRTHS, the numerical model is simulated remotely and the MR damper, as the physical substructure, is tested at Purdue University. The results indicate that dRTHS can be successfully performed, achieving results that are consistent with those of the corresponding single-site RTHS. Lastly, dRTHS is performed to experimentally validate the approach. In these experiments, the numerical model is executed at the remote site, and two physical substructures are located at each site. One MR damper is located at Purdue and a second identical MR damper is located at the University of Connecticut, verifying the proposed framework for dRTHS when multiple physical substructures are involved.

Distributed Real-Time Hybrid Simulation Framework

By leveraging existing capabilities within the earthquake engineering community to conduct RTHS, the development of dRTHS approaches has the potential to address current limitations associated with local laboratory capacities. In this section we introduce a framework that offers the ability to connect geographically distributed physical and computational resources and enable them to be shared across the Internet to conduct a single test.

Description of the dRTHS Framework

In a typical single-site RTHS experiment, the physical and numerical substructures are combined using a transfer system, for example, a servohydraulic actuator, to enforce boundary conditions. The dynamics associated with the presence of that transfer system introduce time lags in the feedback loop (Carrion and Spencer 2007). Time delays are also present owing to communication and computational tasks (Maghareh et al. 2014a). Horiuchi et al. (1999) first demonstrated that time delay in RTHS is equivalent to negative damping in the system. If the time delay is significant and not compensated, the experiment may become unstable (Maghareh et al. 2014a). In dRTHS, the Internet is an additional source of significant time delays. Thus, each of the numerical and physical components is executed locally in real time, whereas data exchanges between those components is delayed by a significant but uncertain amount.

To accommodate network communication time delays for implementation of dRTHS, a modified Smith predictor is used. A generalized dRTHS framework is shown in Fig. 1.

Here the numerical substructure, physical substructure 1, and physical substructure 2 are geographically distributed at two sites, one called the local site and the other called the remote site. The quantities τ_1 and τ_2 are the unknown network time delays in the forward and return paths, respectively. The external excitation D^t (i.e., disturbance) is applied to the numerical substructure, which in turn results in reaction forces in physical substructures 1 and 2. The displacement generated in the numerical substructure, x^t, is transmitted to the remote site over the Internet. The delayed displacement command $x^{t-\tau_1}$ is received by physical substructure 1. The displacement is applied to physical substructure 1, producing a reaction force $f_p(t-\tau_1)$, which is transmitted back to the local site through the network. Finally, with an additional return path network time delay, τ_2, affecting the force signal, the modified Smith predictor is applied to compensate for the network time delay. Then, the compensated physical force, $\widehat{f}_e(t)$, is fed back to the numerical substructure. Because physical substructure 2 communicates with the numerical substructure locally, no significant network time delay is present within the local site.

Modified Smith Predictor

In this study, a Smith prediction–based algorithm was implemented to compensate for the network communication time delays. The Smith predictor is known to be an effective dead-time compensator for systems with predictable pure time delays (Smith 1959). A block diagram of the Smith predictor used herein for dRTHS is shown in Fig. 2(a), which uses an analytical model of the physical substructure in compensating for the network time delay. In Fig. 2, $r(t)$ is the external excitation, $G_n(s)$ is the numerical substructure, $G_p(s)$ is the physical substructure at the remote site, $G_{pm}(s)$ is the prediction model associated with $G_p(s)$, $X(s)$ is the response of the

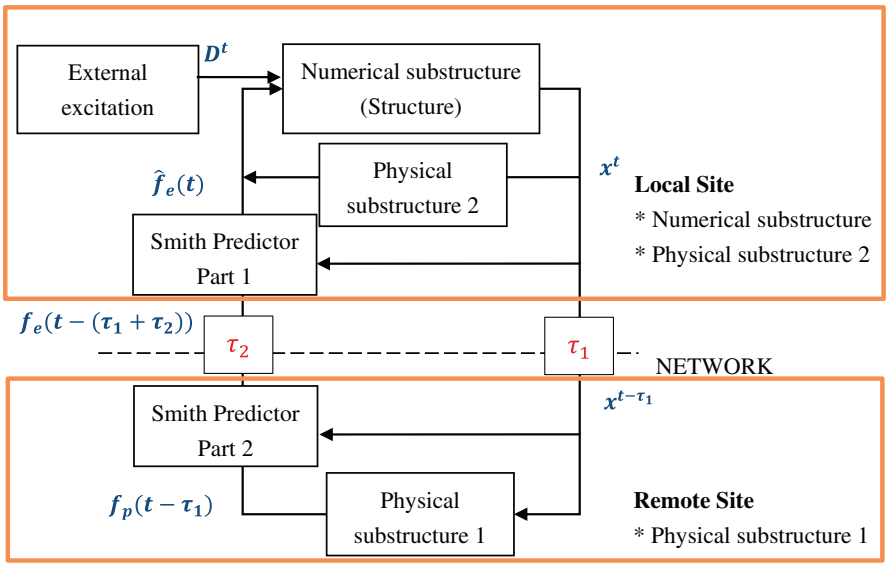

Fig. 1. (Color) Generalized dRTHS framework

numerical substructure, and $f(t)$ is the output of the physical substructure. Because the numerical and physical substructures were geographically distributed, $e^{-\tau_1 s}$ and $e^{-\tau_2 s}$ represent the network time delays actually present in the system, whereas $e^{-\tau_{1p} s}$ and $e^{-\tau_{2p} s}$ are the predicted network time delays. The closed-loop transfer function of the Smith predictor for a linear system is given as:

$$F(s)/r(s) = G_n(s)e^{-\tau_1 s}G_p(s)/[1 + G_n(s)e^{-\tau_1 s}G_p(s)e^{-\tau_2 s} - G_n(s)e^{-\tau_{1p} s}G_{pm}(s)e^{-\tau_{2p} s} + G_n(s)G_{pm}(s)]$$
$$X(s)/r(s) = G_n(s)/[1 + G_n(s)e^{-\tau_1 s}G_p(s)e^{-\tau_2 s} - G_n(s)e^{-\tau_{1p} s}G_{pm}(s)e^{-\tau_{2p} s} + G_n(s)G_{pm}(s)] \quad (1)$$

The Smith predictor represents the plant and network delay exactly when the time delays and known and the prediction model is accurate, that is, when $G_{pm}(s) = G_p(s)$, $\tau_{1p} = \tau_1$, and $\tau_{2p} = \tau_2$. Thus, Eq. (1) reduces to

$$F(s)/r(s) = G_n(s)e^{-\tau_1 s}G_p(s)/[1 + G_n(s)G_p(s)]$$
$$X(s)/r(s) = G_n(s)/[1 + G_n(s)G_p(s)] \quad (2)$$

This general form of the Smith predictor eliminates the network communication delay when the physical substructure is accurately modeled, and the communication network delay is deterministic and constant, and is estimated or measured. However, because of the unpredictable nature of the network traffic and thus the associated time delays, precise prediction of τ_1 and τ_2 was a significant challenge for dRTHS implementation.

To deal with the uncertainty in the delay prediction, a modified version of the Smith predictor was applied and evaluated in this study. This method was proposed to compensate for time delays in wireless sensor network control systems, and was named as the modified Smith predictor (Du and Du 2009). The modified Smith predictor applies multiple Smith predictors for time delay compensation. This system includes a prediction model at the remote site to mask the predictor model for the network delay during transmission across the network. This modified Smith predictor is a real-time dynamic predictor and does not include prediction models of actual network delay, and thus network delays no longer need to be measured, identified or estimated online [Fig. 2(b)]. When the prediction model is accurate, $G_{pm}(s) = G_p(s)$ (i.e., the analytical model is identical to the physical substructure), the signal returned from the remote site to the local site will be 0 in the ideal case when there is no measurement noise. Moreover, the presence of the modified Smith predictor does serve to stabilize the system because it provides a reliable input to use for commanding the local transfer system.

The closed-loop transfer function of the modified Smith predictor is given as:

$$f(s)/r(s) = G_n(s)e^{-\tau_1 s}G_p(s)/\{1 + G_n(s)G_{pm}(s) + G_n(s)e^{-\tau_1 s}[G_p(s) - G_{pm}(s)]e^{-\tau_2 s}\}$$
$$X(s)/r(s) = G_n(s)/\{1 + G_n(s)G_{pm}(s) + G_n(s)e^{-\tau_1 s}[G_p(s) - G_{pm}(s)]e^{-\tau_2 s}\} \quad (3)$$

When $G_{pm}(s) = G_p(s)$, the prediction models can accurately approximate true models and Eq. (3) is reduced to

$$f(s)/r(s) = G_n(s)e^{-\tau_1 s}G_p(s)/[1 + G_n(s)G_p(s)]$$
$$X(s)/r(s) = G_n(s)/[1 + G_n(s)G_p(s)] \quad (4)$$

As seen from Eq. (4), the uncertain communication network delays present in the forward and return paths are removed from the closed-loop system for $X(s)$. As a result, the network delays do not need to be measured or identified in real time during the data transmission process, which reduces the requirement of clock synchronization of these two sites. However, the need for data arriving in the correct sequence will be important.

As shown in Fig. 1, the modified Smith predictor uses two identical analytical models representing physical substructure 1: (1) Smith predictor part 1 at the local site, and (2) Smith predictor part 2 at the remote site. An estimate of the current physical restoring force, $\hat{f}_e(t)$, is provided as

$$\hat{f}_e(t) = f_{pm}(t) + f_e[t - (\tau_1 + \tau_2)] = f_{pm}(t) + \{f_p[t - (\tau_1 + \tau_2)] - f_{pm}[t - (\tau_1 + \tau_2)]\} \quad (5)$$

where $f_{pm}(t)$ = analytically predicted restoring force of the physical substructure at time t; $f_p(t)$ = measured restoring force

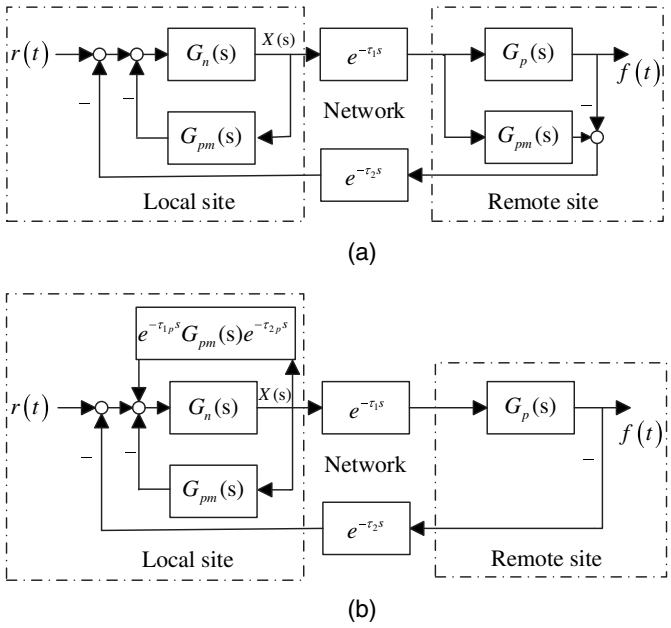

Fig. 2. Block diagram of (a) general Smith predictor and (b) modified Smith predictor use in dRTHS

of the physical substructure at time t; $f_e[t-(\tau_1+\tau_2)]$ = force error between the measured restoring force of the physical substructure and the predicted restoring force; and $\widehat{f}_e(t)$ = estimated physical force at the current time. The variables τ_1 and τ_2 are the network time delays in the forward path and return path, respectively.

Hardware Setup and Network Communication Protocol

An overview of the hardware setup is shown in Fig. 3. Mathwork's *xPC Target* was used at both the local and remote sites as the real-time operating system. Each *xPC Target* computer required two Ethernet boards, one was used for host-target communication, and the second one was dedicated to real-time data transmission to the remote site's *xPC Target* over the Internet. Each *xPC Target* worked with one xPC host. The Simulink model compiled by the *Simulink Coder* on the xPC Host was uploaded to the target computer via a transmission control protocol/Internet protocol (TCP/IP) communication link for execution.

At the local site, the code included the numerical substructure, hydraulic actuator control algorithms for physical substructure 2, and modified Smith predictor part 1. This code was compiled on the xPC Host and downloaded to the local *xPC Target* for execution. At the remote site, the code included the hydraulic actuator control algorithms for physical substructure 1 and modified Smith predictor part 2. This code was compiled on the xPC Host and executed on the remote target PC. Using both xPC targets, the actuator command was sent to the respective servohydraulic controller [which implemented an inner-loop proportional–integral–derivative (PID) controller] to enable high-precision motion control of the hydraulic actuators and to compensate for the dynamics of each transfer system. The sensor measurements from physical substructures were fed back to the *xPC Target* machines. Data transmission between the two *xPC Target* machines at the local and remote sites was performed over the Internet.

Here, we aimed to conduct successful dRTHS in the presence of a significant network communication delay in the transmission of data between geographically distributed sites. The prediction model was unlikely to be perfect in most cases. Thus, any modeling errors between the model and physical system would degrade the estimates of reaction forces. Because minimization of the delay would be important for the success of a dRTHS, even with compensation, it was desirable to adopt a low-latency protocol. Transmission control protocol is one of the most commonly used protocols, and is normally regarded as quite reliable because it has error-checking and correction features. Transmission control protocol guarantees data delivery and also assures that packets are delivered in the same order that they were sent. However, TCP is greatly affected by network dynamics, and variations in transmission rates are subject to network capacity. Thus, this option may result in significant delays in data delivery which is impractical for this application. User datagram protocol (UDP) is a communication protocol that allows individual packets to be individually routed at every time step and is often used in applications aimed toward real-time operation, such as voice over internet protocol (VoIP). However, with unusually heavy traffic it is possible that packet ordering may be affected, in which data segments might arrive out of sequence. This effect was not observed in these experiments, but is possible. Ojaghi et al. (2014) demonstrated that UDP is preferable to TCP for dRTHS. The network time delays observed between Purdue and UConn (approximately 1,400 km apart) were typically approximately 35–45 ms when UDP/IP communication was used, as shown in Fig. 4. The network time delay increased to approximately 100–120 ms when using TCP for data transfer. To achieve a high network performance, UDP/IP was applied in our hardware setup. Note that no great measures were taken here to enhance cyber security, although in the future research in this important topic should be pursued. A virtual-private network (VPN) may be used, although it would likely add to the network time delays.

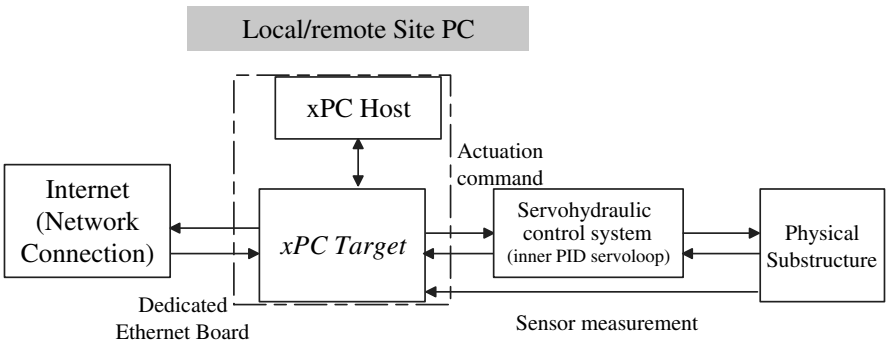

Fig. 3. Hardware setup for dRTHS

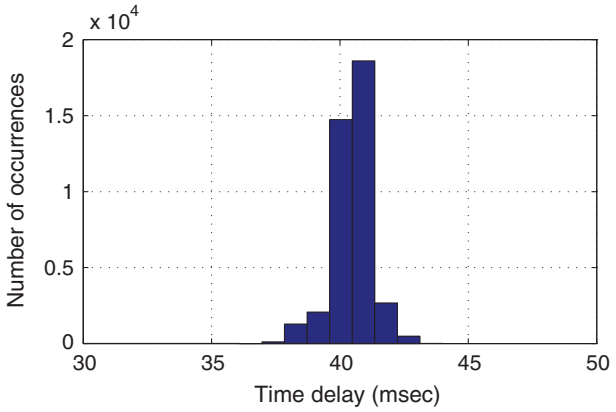

Fig. 4. (Color) Histogram of the measured transmission delay between Purdue and UConn

Study of Sensitivity to Network Time Delays and Modeling Errors

Prediction models of the physical substructures used in the dRTHS must be used to develop and implement the modified Smith predictor. Thus, analytical models of the physical substructures must be developed or identified, which often contain complex nonlinear dynamics and modeling errors. The presence of uncertain network time delays may also impair the ability of the Smith predictor to compensate for such delays. Thus, the sensitivity of the dRTHS framework to network delay and modeling errors is examined here through a parametric study. In this study, all of the physical substructures were replaced with idealized numerical models, that is, virtual dRTHS was used. This approach facilitated isolation of the factors that could influence the results, to focus on known modeling errors and network time delays. Sensor noise did not play a role in these sensitivity studies, for example. Models of the physical substructure were adjusted in these studies such that they overpredicted or underpredicted the forces generated (as compared to the nominal models), and thus induced modeling errors. However, the prediction models used for implementation of the Smith predictors were based on specific nominal model parameters. Two cases were considered: (1) a linear case based on a spring; and (2) a nonlinear case based on a MR damper.

Setup for Sensitivity Study

The structure considered in this study consisted of a seismically excited, two-story structure with an auxiliary linear or nonlinear device placed between the ground and the first story. The equations of motion of a linear-elastic structure subjected to a ground motion are given by

$$M_s\ddot{X} + C_s\dot{X} + K_sX = \Lambda f - M_s\Gamma\ddot{X}_g \tag{6}$$

where f = measured device force vector ($L \times 1$); X = vector of displacements of the structure relative to ground ($N \times 1$); M_s = mass matrix ($N \times N$); C_s = damping matrix ($N \times N$); K_s = stiffness matrix ($N \times N$); Λ = damper influence matrix ($N \times L$); and Γ = column vector of ones ($N \times 1$). The number of floors of the structure is depicted by N, and the number of damper devices applied to the structure is depicted by L.

The state-space form of Eq. (6) can be written

$$\dot{z} = Az + B\begin{bmatrix}\ddot{x}_g \\ f\end{bmatrix} \tag{7}$$

$$y = Cz + D\begin{bmatrix}\ddot{x}_g \\ f\end{bmatrix} \tag{8}$$

where z = state vector; and y = vector of measured outputs. Matrices A and B are defined as

$$A = \begin{bmatrix}0 & I \\ -M_s^{-1}K_s & -M_s^{-1}C_s\end{bmatrix}, \qquad B = \begin{bmatrix}0 & 0 \\ M_s^{-1}\Lambda & -\Gamma\end{bmatrix} \tag{9}$$

As shown in Fig. 5, the two-story structure is simulated as a numerical substructure whereas the auxiliary device is regarded as the simulated physical substructure. To realistically examine dRTHS with the modified Smith predictor, the numerical substructure and simulated physical substructure were executed separately on two *xPC Targets*.

The structure considered in this study was a two-story shear frame with lumped masses and rigid beams used in past dRTHS

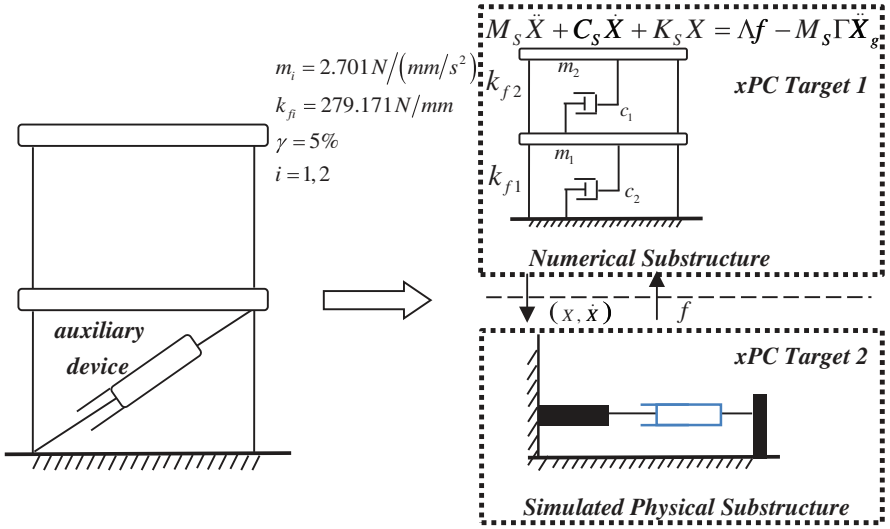

Fig. 5. (Color) Example structure of dRTHS for sensitivity study

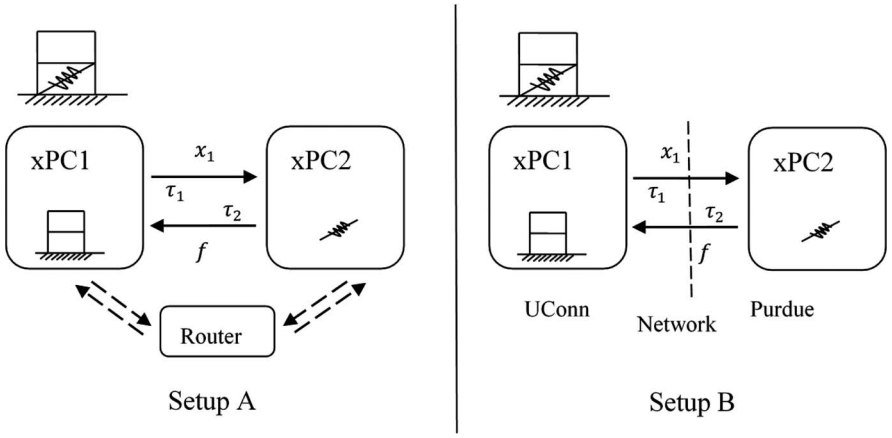

Fig. 6. Setups for the sensitivity study

studies (Kim et al. 2012). The frame was modeled as a two-degree-of-freedom system. The natural frequencies were 1.00 and 2.62 Hz for the first and second modes, respectively. Modal damping ratios of 5% were assumed for each mode. The mass, stiffness, and damping matrices are shown in Eq. (9), where the units are Newton and millimeter.

$$M_s = \begin{bmatrix} 2.701 & 0 \\ 0 & 2.701 \end{bmatrix} \text{N}/(\text{mm}/\text{s}^2)$$
$$C_s = \begin{bmatrix} 3.684 & -1.228 \\ -1.228 & 2.456 \end{bmatrix} \text{N}/(\text{mm}/\text{s})$$
$$K_s = \begin{bmatrix} 558.343 & -279.171 \\ -279.171 & 279.171 \end{bmatrix} \text{N}/\text{mm} \quad (10)$$

The record of the 1940 El Centro earthquake was used as the external excitation (ground motion). The original record had the peak ground acceleration of 3.41 m/s^2. However, the record was scaled down by a factor of 5 owing to the stroke limitations of the hydraulic actuator serving as the transfer system.

Two setups were used here, denoted setup A and setup B, as shown in Fig. 6. In setup A, two *xPC Target* computers were implemented at the same site by connecting to the same router. This setup was used to enable the introduction of a known (induced) time delay. *xPC Target* 1 (xPC1) executed the model of the two-floor structure and modified Smith predictor part 1 in real time, and *xPC Target* 2 (xPC2) executed the analytical model of the physical substructure and modified Smith predictor part 2. The two target computers communicated with each other and exchanged data through Ethernet cards. A network time delay was artificially introduced in the xPC code, but was constant over the duration of each simulation. In a suite of simulations, the value of the delay was varied from 0 to 100 m to examine the impact of these delays on the performance. In setup B, two *xPC Target* computers were distributed between Purdue and UConn, respectively. In this dRTHS configuration, the network time delay was variable and unknown owing to changing network conditions.

Linear Case

In the linear case study, the physical substructure consisted of a supplemental spring. The spring was numerically modeled using the equation

$$f = k_s x_1 \quad (11)$$

where k_s = stiffness of the spring and the nominal value is $k_s = 20\% k_f$, where k_f = stiffness of the first floor of the structure; and x_1 = displacement at the first story. Additionally, in the linear case, the same type of analytical model for the linear spring was used for both the physical specimen and for the prediction model used in the Smith predictor. To induce modeling errors in the Smith predictor, the stiffness of the spring prediction model was multiplied by a gain simulating both overprediction and underprediction of the spring force by 10, 20, and 30%.

Fig. 7 shows the sensitivity of the example case using this framework to both network time delays and modeling error in setup A. A linear relationship was observed between peak displacement error and network time delay, and the peak displacement error increased as the network time delay grew. Note that the error was 0% when no modeling error was present, although the network delay varied from 0 to 100 ms. This result demonstrated that the modified Smith predictor did eliminate network communication delay when the prediction model accurately represented the physical substructure. There was a characteristic relationship between the magnitude of modeling error and the network time delay. As the modeling error increased from 10 to 30%, the peak displacement increased. Fig. 7 shows that with a modeling error of 30% and a network delay of 50 m, a modest second-floor peak error of 6.5% was achieved for this particular structure. Fig. 8 shows the structural response to model error when the network delay is 50 m

Fig. 9 shows the sensitivity of setup B to modeling errors, considering realistic network conditions between Purdue and UConn, in which the actual time delay was observed in the distributed real-time test. In Fig. 9, the dashed line represents the upper bound of the peak displacement error. The upper bound is defined as the error present when the same overprediction or underprediction spring model is used to perform a pure computational simulation. The solid line is the peak displacement error to modeling error when the erroneous spring model is used in a distributed simulation (setup B). Degradation occurred when the predictor model deviated from the physical plant. However, the absolute value of the peak displacement error generated in setup B was consistently lower than the value in upper-bound case for any level of modeling error. When a reasonable prediction model was available, global responses obtained through dRTHS were found in this case to be more accurate than a pure numerical simulation. Thus, dRTHS may be preferred to a pure numerical simulation if the model of the physical substructure was truly unknown. As observed in Fig. 9, an average network delay between Purdue and UConn estimated at

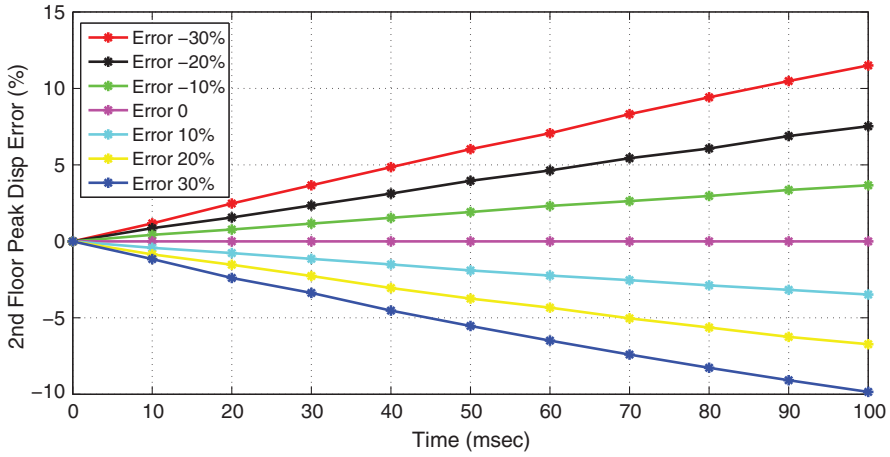

Fig. 7. (Color) Peak displacement error to model error in setup A in linear case

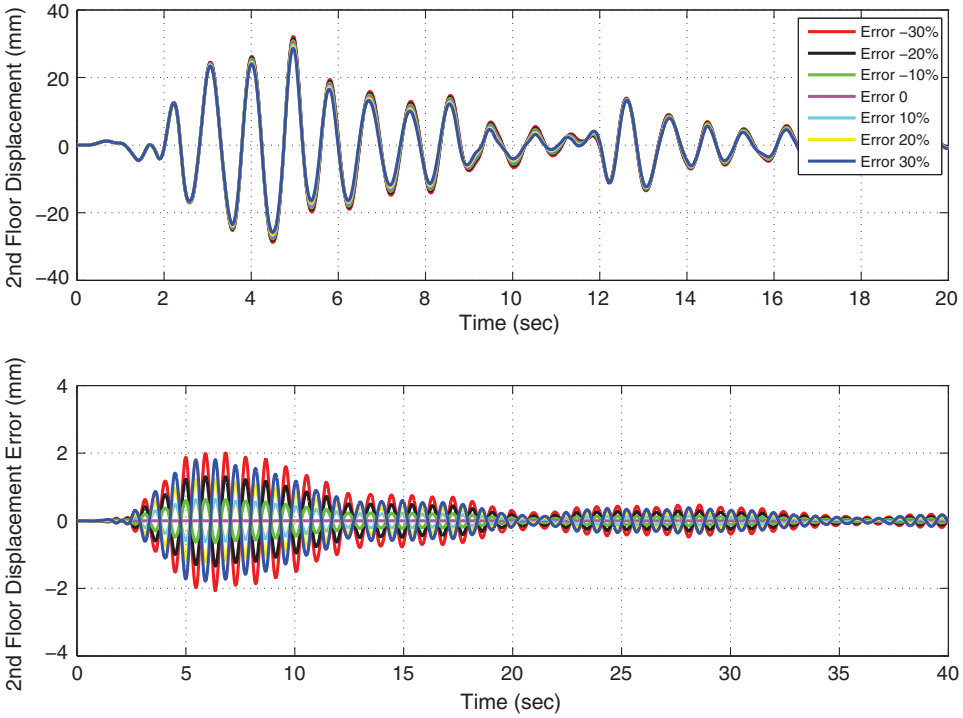

Fig. 8. (Color) Representative structural response to modeling errors (with a 50-ms delay) in setup A corresponding to the linear case

41 ms resulted in a peak displacement error of 4.3% for a modeling error of ±30%.

Nonlinear Case

In the linear case, the sensitivity of the system to modeling errors and time delays was relatively predictable. Next, a nonlinear case study was conducted to understand the sensitivity of this approach to network time delays and modeling errors. Here the physical substructure consisted of a MR damper placed between the ground and first floor. A phenomenological Bouc-Wen model (Fig. 10) developed by Spencer et al. (2004) for a MR damper was used for both the simulated physical specimen and the prediction model.

The force generated by the MR damper was

$$F = \alpha z + c_0(\dot{x} - \dot{y}) + k_0(x - y) + k_1(x - x_0) \qquad (12)$$

where the evolutionary variable z was governed by

$$\dot{z} = -\gamma|\dot{x} - \dot{y}|z|z|^{n-1} - \beta(\dot{x} - \dot{y})|z|^n + A(\dot{x} - \dot{y}) \qquad (13)$$

The applied voltage, the viscous damping constants, α, c_0, and c_1, were given by the following linear functions of current input u:

$$\alpha = \alpha(u) = \alpha_a + \alpha_b u, \qquad c_0 = c_0(u) = c_{0a} + c_{0b}u,$$
$$c_1 = c_1(u) = c_{1a} + c_{1b}u, \qquad \dot{u} = -\eta(u - v) \qquad (14)$$

where v = voltage applied to the current driver.

A total of 14 parameters were needed to simulate the behavior of the MR damper. To mimic an overprediction or underprediction modelling error in the MR damper for a sensitivity study, the parameters α_a and α_b, which directly affected the magnitude of the yield force of the MR damper and thus had the most dramatic

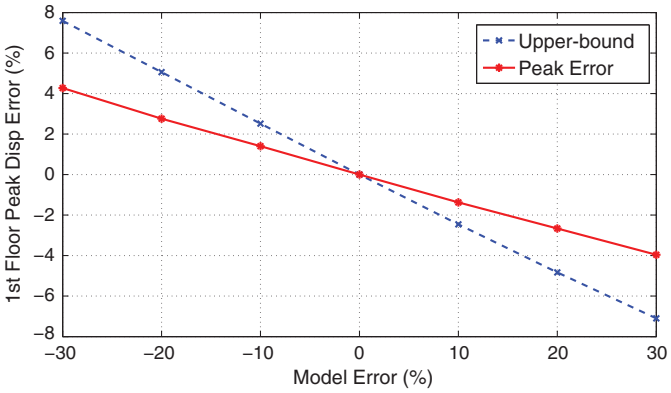

Fig. 9. (Color) Sensitivity to network time delay and modeling error in setup B—spring case

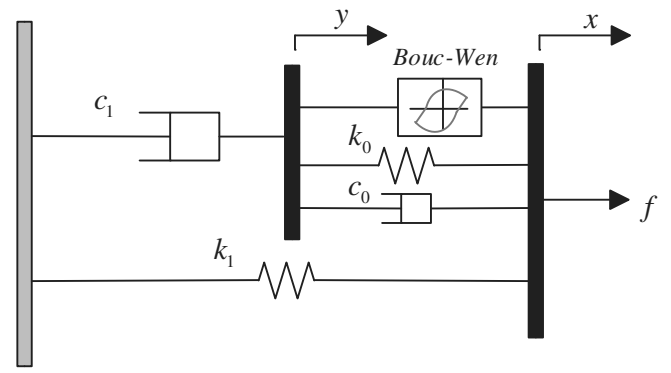

Fig. 10. Phenomenological Bouc-Wen model for MR damper

Table 1. Magnetorheological Damper Model Parameters of Physical Substructure Model A (Nominal Model)

Parameter	Value
α_a (N/cm)	35.84
α_b (N/cm/V)	83.04
c_{0a} (N · s/cm)	1.539
c_{0b} (N · s/cm/V)	32.82
k_0 (N/cm/V)	5.86
γ (cm^{-2})	3.62
β (cm^{-2})	3.62
A	154.60
k_1 (N/cm)	0.016
c_{1a} (N · s/cm)	99.47
c_{1b} (N · s/cm/V)	403.86
η (s^{-1})	60
x_0 (cm)	0

impact on errors in the model, were varied in the prediction model to study the sensitivity of the Smith predictor to modeling errors in the nonlinear component.

Identified parameters of the Bouc-Wen model were given as physical substructure model A in Table 1 (Gao 2012). These values were used in the nominal model. To simulate overprediction or underprediction of the MR damper force, six different models, B1–B6, listed in Table 2, were used in the modified Smith predictor, yielding a RMS error of force varying from −30 to +30% at 10% increments, when damper was subjected to a 2.5-Hz sine wave displacement with the amplitude of 5 mm and constant voltages of 0 V (passive off) and 3 V (passive on). The normalized RMS force error was calculated as in Eq. (14). The values of α_a and α_b were varied in models B1–B6 and the value of the remaining 12 parameters in models B1–B6 used the values in the nominal model A. The comparison between physical specimen model A and prediction models B1–B6 are presented in Fig. 11.

$$E_f = \text{sgn}[\max(f_{B,i}) - \max(f_{A,i})] \cdot \sqrt{\frac{\frac{1}{N}\sum_{i=1}^{N}(f_{B,i} - f_{A,i})^2}{\frac{1}{N}\sum_{i=1}^{N}(f_{A,i})^2}} \times 100\% \quad (15)$$

Fig. 12 shows the sensitivity of the framework to changes in network delay and modeling error in setup A, as measured by the error in the second-floor peak displacement of the building in passive-off and passive-on cases. The peak displacement error increased as the network time delay increased. Note that the peak error was 0% when the modeling error was 0% although network delay varied from 0 to 100 ms in both the passive-off and passive-on cases. It should be noted that the larger the influence of the physical substructure on the numerical substructure, the larger the peak displacement error, as observed by the increasing damper force of passive-on case. As seen for the B1 model when time delay was 100 ms, the resulting peak displacement error was approximately 0.29 and 3.75% for the passive-off and passive-on cases, respectively. Fig. 12 shows that for a modeling error of 30% and a network delay of 50 ms, a modest second-floor displacement peak error of 3.75% was observed.

The results clearly showed that there was a nonlinear relationship between the peak displacement error and the network time delay in the nonlinear case. This occurred because the Bouc-Wen equations modeled the nonlinear hysteretic MR damper, which produced a variety of hysteretic patterns with varying maximum force levels. Although the values of α_a and α_b, which directly affected the magnitude of the force, were varied symmetrically in the prediction model, the overall model behavior was nonlinear, and thus the resulting impact was not symmetric in the closed-loop system. Thus, the resulting peak errors in Figs. 12 and 13 were not symmetric. Researchers should consider the sensitivity of their particular models to minimize the effect of modeling errors when conducting a given dRTHS experiment.

Fig. 13 shows the sensitivity of the example case to modeling errors under real network conditions, in which the actual time delay was observed in the distributed real-time test. As in the linear case, the solid line shows the upper bound of the peak displacement error, where the overprediction or underprediction MR damper models B1–B6 were used in pure computational simulation. The dashed line is the resulting peak displacement error to modeling error when the erroneous MR damper model was used to implement the modified Smith predictor (setup B). Again, the absolute value of peak displacement error generated in setup B was consistently lower than error with pure simulation for any level of

Table 2. Magnetorheological Damper Model Parameters Simulating Modeling Errors

Parameters	Nominal value (model A)	B1 (RMS −30%)	B2 (RMS −20%)	B3 (RMS −10%)	B4 (RMS 10%)	B5 (RMS 20%)	B6 (RMS 30%)
α_a (N/cm)	35.84	22.35	26.70	31.00	40.84	45.84	51.00
α_b (N/cm/V)	83.04	48.00	59.00	70.00	93.60	104.50	116.50

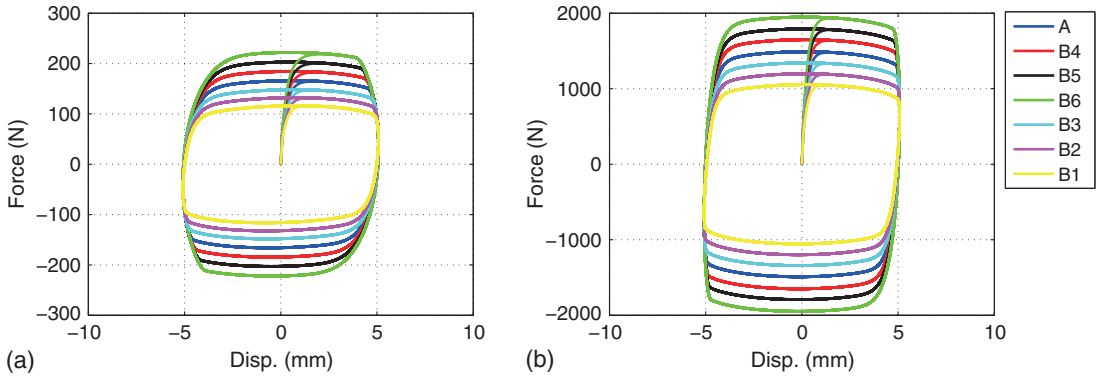

Fig. 11. (Color) Response of MR damper model to a steady-state 5-mm, 2.5-Hz sinusoidal excitation: (a) passive off; (b) passive on

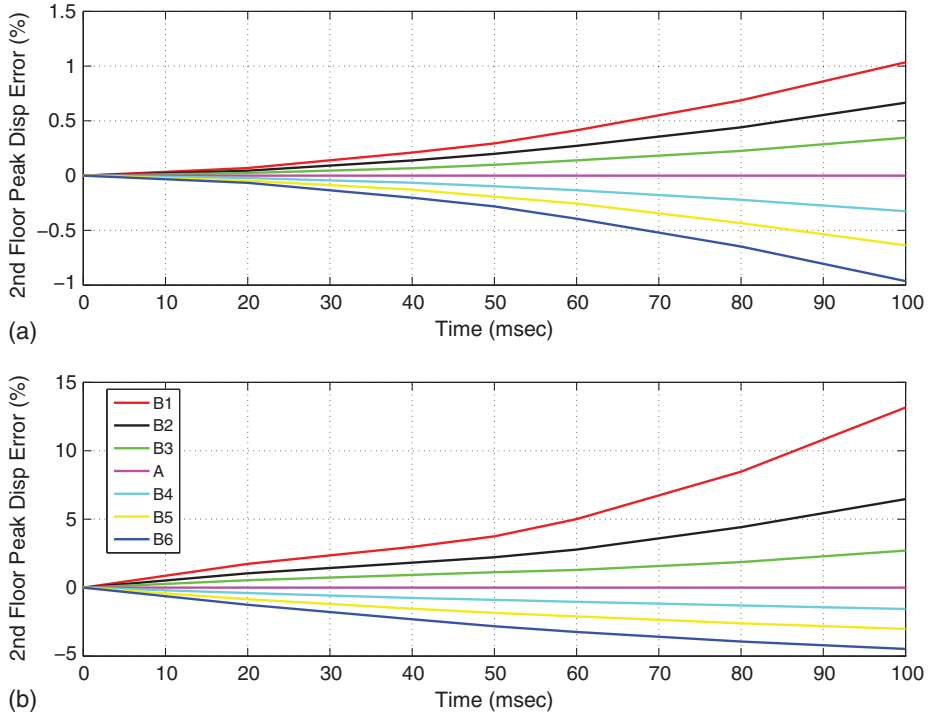

Fig. 12. (Color) Peak displacement error to model error in setup A in nonlinear case: (a) passive off; (b) passive on

modeling error. Thus, although degradation did occur, if the analytical model was unknown, dRTHS was preferred for examining the global response of the system.

As observed in Fig. 13, the peak error was 0% when an identical analytical model was applied in modified Smith predictor and in the computational simulation. A peak error of 1% in passive-off case and a peak error of lower than 5% for passive-on case was achieved with modeling errors of 30% (B6 model) and −30% (B1 model).

The results of these parameters studies demonstrate the feasibility of this dRTHS framework under realistic network conditions. The modified Smith predictor is mainly useful for dRTHS when there is some understanding of the behavior of the specimen. And, as shown here, the Smith predictor can be used effectively when the model parameters are uncertain, although a reasonable model is clearly needed. As seen in both the linear and nonlinear cases considered here, the sensitivity to errors in the model does depend on the building model, and, in turn, the partitioning choices made to establish numerical and physical substructures. Note that the influence of partitioning choices in RTHS has been investigated in the past (Maghareh et al. 2014a) and these results support the conclusions of that work. This type of sensitivity analysis serves as a guideline prior to conducting any dRTHS to understand the performance of system and to examine the ability and sensitivity of the modified Smith predictor.

Experimental Verification of dRTHS Framework

A series of experiments were conducted between Purdue and UConn to verify the dRTHS framework and demonstrate its effectiveness experimentally. Three experimental configurations with increasing levels of complexity were considered for this verification, as illustrated in Fig. 14. In Case I, a single-site RTHS involved the same numerical substructure, and, as the physical substructure, a servohydraulic actuator with a servocontroller and a nonlinear

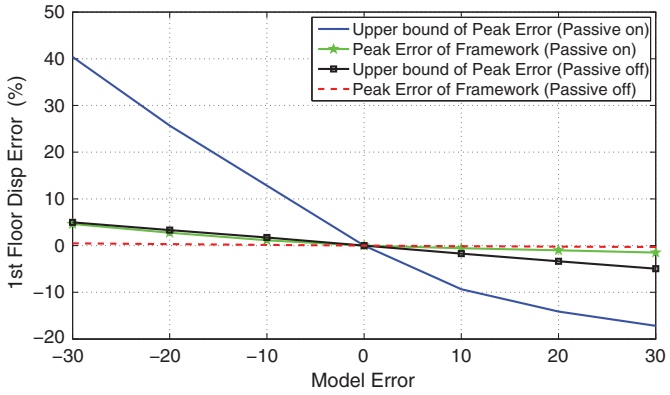

Fig. 13. (Color) Peak displacement error to time delay and model error in setup B (nonlinear case)

MR damper. In Case II, dRTHS was conducted using the proposed framework with the numerical substructure at UConn and the nonlinear physical substructure connected to the hydraulic actuator at Purdue. To verify the performance of dRTHS framework, experiments considering Case II were compared with those of Case I (single-site RTHS). In Case III, a more complex dRTHS was considered, and two similar nonlinear physical substructures (MR dampers) were geographically distributed.

The numerical substructure used in all cases was the building model used in sensitivity analysis, a two-story shear frame with lumped masses and rigid beams, subjected to ground motion in one direction. Here, the structure was subjected to an El Centro earthquake record scaled to 20% owing to the stroke limitation of the transfer system. The mass, stiffness, and damping matrices are provided in Eq. (10). In each case, the MR damper(s) acted as the physical substructure(s). A RD-8041-1 MR damper manufactured by Lord Corporation (Cary, North Carolina) was used at Purdue. The specified peak-to-peak damper force was 2.4 kN when subjected to a velocity of 5 cm/ sec at 1 amp current input. The MR damper at UConn was a RD-8041-1 MR damper manufactured by Lord Corporation. A Lord Corporation Wonder Box device provided the necessary current to drive the MR damper, operating as an interface device to control the MR damper. The output current with the Wonder Box was 0.0 amp when the control input was below 0.6 V, and was linearly proportional to the input voltage until the saturation level was reached.

Distributed RTHS Implementation

Implementation of the dRTHS included a numerical substructure, physical substructure, digital signal processor, servohydraulic actuator with servocontroller, and a network connection. The physical substructure configuration in the dRTHS framework for Case II and Case III is shown in Fig. 15, in which Case III included the grey region at UConn site.

xPC Target was used as the real-time operating system at both Purdue and UConn. A Simulink model of numerical substructure, Smith predictor, and actuator motion controller were developed and compiled on the host PC. Then these compiled models were downloaded to the target PC(s) for execution on the target xPC(s). Communication between the host and target PC was realized via Internet at a rate of 1,024 Hz. The target PCs at Purdue and UConn communicated with each other through the UDP/IP protocol over dedicated network boards.

At Purdue, in all configurations a Speedgoat/xPC (Speedgoat GmbH, Natick, Massachusetts) real-time kernel was used as the target PC, equipped with an 18-bit analog National Instruments model 112 I/O board (National Instruments Corporation, Austin, Texas). This board supports up to 32 differential simultaneous A/D channels and 8 D/A channels, with a minimum I/O latency of lower than 5 μs for all channels. The external command was applied with the Speedgoat/xPC. The inner PID control loop for the actuator was provided with the Shore Western SC6000 (Shore Western Manufacturing, Monrovia, California) which implemented using the internal LVDT and load cell. This hydraulic system provided maximum load capacity of 10 kN and a stroke of 0.15 m. The MR damper was driven by the hydraulic actuator which was controlled by the servocontroller in displacement feedback mode. The RIAC algorithm was implemented to compensate for the dynamics of the local transfer system (Ou et al. 2015).

In Case III, which included the remote UConn site, the system was controlled using a Q8 Multi-Q board (Quanser, Markham, Ontario, Canada) which included an inner PID servoloop. The command signal to control the behavior of the MR damper was generated by the Q8 Multi-Q board. The resulting damper force was measured with a PCB Piezotronics force transducer model 208C01 (PCB Piezotronics, Depew, New York).

For dRTHS implementation, responses were sampled at a rate of 1,024 Hz, and numerical simulation of the building model was performed using Runge-Kutta method of numerical integration.

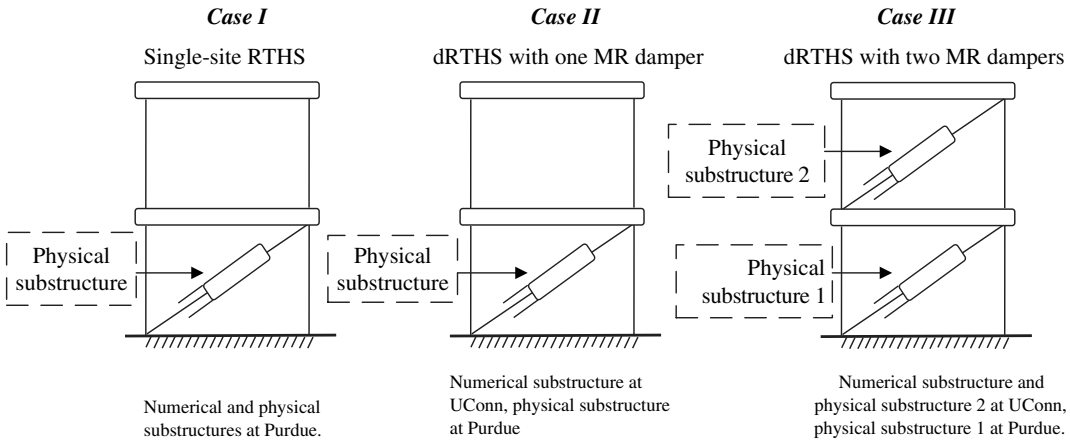

Fig. 14. Real-time hybrid simulation configurations considered for experimental verification

J. Comput. Civ. Eng., 2017, 31(4): 04017014

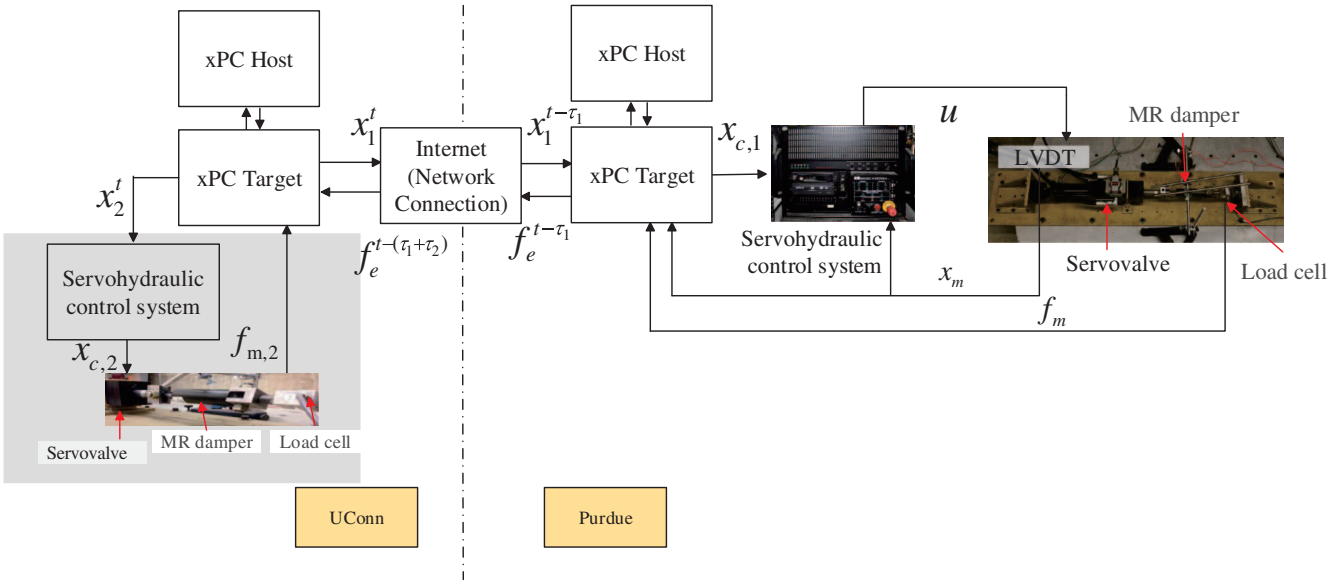

Fig. 15. (Color) Physical substructure configurations in Cases II and III

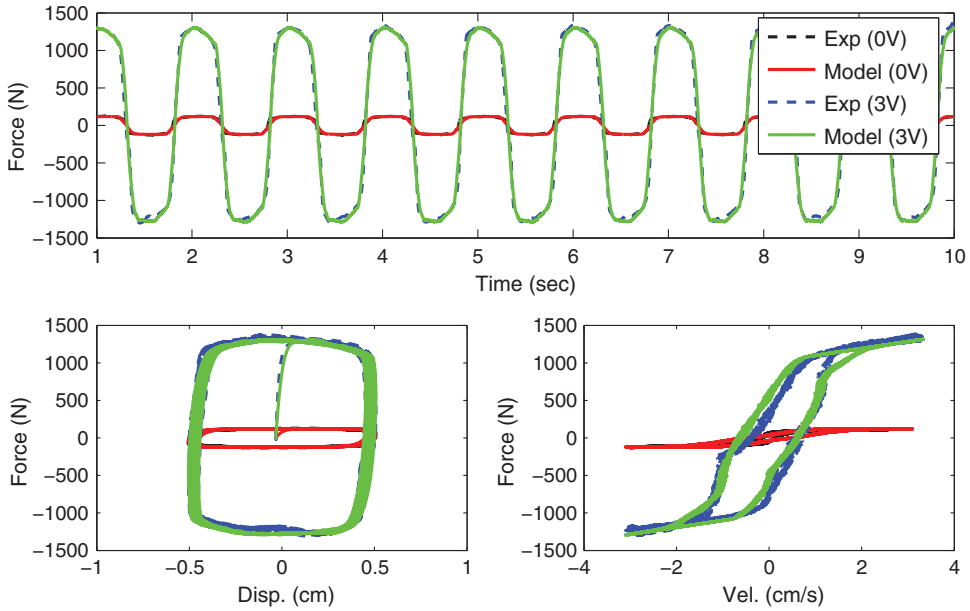

Fig. 16. (Color) Responses of identified Bouc-Wen model and experimental data

Magnetorheological Damper Model Identification

In Case II, the physical substructure (MR damper) and the numerical substructure were geographically distributed at Purdue and UConn, respectively. In Case III, physical substructure 1 (MR damper at the first floor) was located at Purdue (remote site) whereas the numerical substructure and physical substructure 2 (MR damper at the second floor) were located at UConn (local site). As discussed previously, the modified Smith predictor, which included the two analytical models of physical substructure 1, was applied to compensate for network time delays. For optimum performance of the modified Smith predictor, a mechanical model of the MR damper at Purdue site was identified before conducting experiments for Cases II and III.

A phenomenological Bouc-Wen model, with parameters identified based on sinusoidal characterization tests, was used to construct the prediction model for the MR damper. The form of the Bouc-Wen model used for this class of MR dampers is provided in Eq. (12). To identify the parameters, the MR damper located at Purdue was tested using a 1-Hz (which is the natural frequency of the numerical substructure for the first mode) sine wave with an amplitude of 5 mm and constant external voltages of 0 and 3 V. The parameters of the model were then obtained through a standard nonlinear constrained optimization (*lsqcurvefit*) available in *MATLAB* to identify the best parameters to represent the experimental data using the typical procedure for such model identification (Gao 2012). A comparison between the experimental results and the identified Bouc-Wen model response is shown in Fig. 16 indicating good agreement at both voltage levels. The identified parameters of the Bouc-Wen model are given in Table 3.

Table 3. Identified Bouc-Wen Model Parameters for Purdue Damper

Parameters	Value
α_a (N/cm)	25.32
α_b (N/cm/V)	69.70
c_{0a} (N · s/cm)	1.54
c_{0b} (N · s/cm/V)	32.82
k_0 (N/cm/V)	5.86
γ (cm^{-2})	3.62
β (cm^{-2})	3.62
A	154.60
k_1 (N/cm)	0.016
c_{1a} (N · s/cm)	99.47
c_{1b} (N · s/cm/V)	403.86
η (s^{-1})	60
x_0 (cm)	0

Discussion of Results

To evaluate the approach, a comparison is first made between the results in Cases I and II, which serves to confirm that the dRTHS configuration yields essentially the same results, and verifies the performance of the framework. Next, an evaluation of the dRTHS system with two physical substructures is conducted, and the performance of the structural control system is examined.

Comparison of Single-Site and Distributed Results

Two control cases of RTHS tests were conducted for both single-site RTHS (Case I) and dRTHS (Case II) with one MR damper on the first floor: (1) passive-off control with a constant 0 V, and (2) passive-on control with a constant 3 V. The comparison between Case I and Case II serves to evaluate the performance of the proposed dRTHS framework. The results of Case II are compared to those of Case I where network delay is not present. Peak responses and performance indicators are summarized in Table 4. To quantitatively compare the results of the two systems, the following evaluation metrics are computed for each of the responses of interest:

$$J_{\text{Peak}} = \left| \frac{\max(r_{\text{II}}) - \max(r_{\text{I}})}{\max(r_{\text{I}})} \right| \times 100\% \tag{16}$$

$$J_{\text{RMS}} = \frac{\text{rms}(r_{II} - r_I)}{\max(r_{\text{I}}) - \min(r_{\text{I}})} \times 100\% \tag{17}$$

$$\rho_{I,\text{II}} = \frac{\sum_1^n (r_{\text{I}} - \frac{1}{n}\sum_1^n r_{\text{I}})(r_{II} - \frac{1}{n}\sum_1^n r_{\text{II}})}{\sqrt{\sum_1^n (r_{\text{I}} - \frac{1}{n}\sum_1^n r_{\text{I}})^2}\sqrt{\sum_1^n (r_{\text{II}} - \frac{1}{n}\sum_1^n r_{\text{II}})^2}} \tag{18}$$

$$\text{SD} = \sqrt{\frac{1}{n}\sum_1^n \left(r_i - \frac{1}{n}\sum_1^n r_i\right)^2} \tag{19}$$

where r_{I} = particular response of Case I; and r_{II} = corresponding response of Case II.

As seen in Table 4, in the passive-off case, the 1st-floor peak displacement in Cases I and II are 16.34 and 16.31 mm, respectively. The 2nd-floor peak displacement in Cases I and II are 25.07 and 24.95 mm, respectively. Observed differences in both the measured displacements and forces between the dRTHS (Case II) and the single-site RTHS (Case I) are negligible. The difference in the RMS values of the 1st-floor displacement and damper forces between Cases II and I are 0.36 and 13.57%, respectively. For the passive-on case, the 1st-floor peak displacement of the Cases I and II are 6.10 and 6.13 mm, respectively. The maximum MR damper force for Cases I and II are 1,452.2 and 1,515.6 N. The normalized error in the peak responses for the displacement and force are 0.56, 4.36%. The difference in the RMS values of the displacement and damper force between Cases I and II are 1.42 and 5.13%, respectively. The correlation coefficients of 1st-floor and 2nd-floor displacement and damper forces between Cases II and I are around 1, indicating the strong relationship between Cases I and II. Standard deviation (SD) values here are for comparative purpose of the responses through time history. SD values of each case are similar, therefore the responses through all time history in Case II shows a good agreement with those in Case I.

Fig. 17 shows the displacement response of the structure and measured MR damper force during the earthquake for passive-on control. Note that in Case II, the MR damper force has an abrupt decrease at the peaks of displacement to compensate the influence of network delay. However, the MR damper force adjusts to the appropriate peak value quickly, as in Fig. 17. Thus, the difference in RMS value of damper force is relatively large compared with that of displacement. The MR damper generated a peak force value basically around a displacement value of 0 mm owing to the dynamic characteristics of the MR damper and as such the difference in response of displacement is less affected by the difference of response of force. Therefore, the displacement response is quite similar between Cases I and II whereas the difference in damper force is somewhat larger. The displacement and force as a function of time, as well as the force-displacement responses for the passive-on case show good agreement between Cases I and II as illustrated in Fig. 17.

Table 4. Peak Responses and Associated Performance Indicators

	Case I			Case II		
Evaluation index	First-floor displacement (mm)	Second-floor displacement (mm)	MR damper force (N)	First-floor displacement	Second-floor displacement	MR damper force
Passive off						
Peak value	16.34	25.07	217.8	16.31 mm	24.95 mm	216.9 N
J_{Peak}	—	—	—	0.47%	0.48%	0.43%
J_{RMS}	—	—	—	0.36%	0.68%	13.6%
$\rho_{\text{I,II}}$	—	—	—	0.9996	0.9997	0.8585
SD	4.05	6.64	106.2	4.05 mm	6.65 mm	104.9 N
Passive on						
Peak value	6.10	12.56	1452.2	6.13 mm	12.96 mm	1515.6 N
J_{Peak}	—	—	—	0.56%	0.32%	4.36%
J_{RMS}	—	—	—	1.42%	2.75%	5.13%
$\rho_{\text{I,II}}$	—	—	—	0.9928	0.9964	0.9084
SD	1.49	3.16	616.4	1.43 mm	3.30 mm	599.1 N

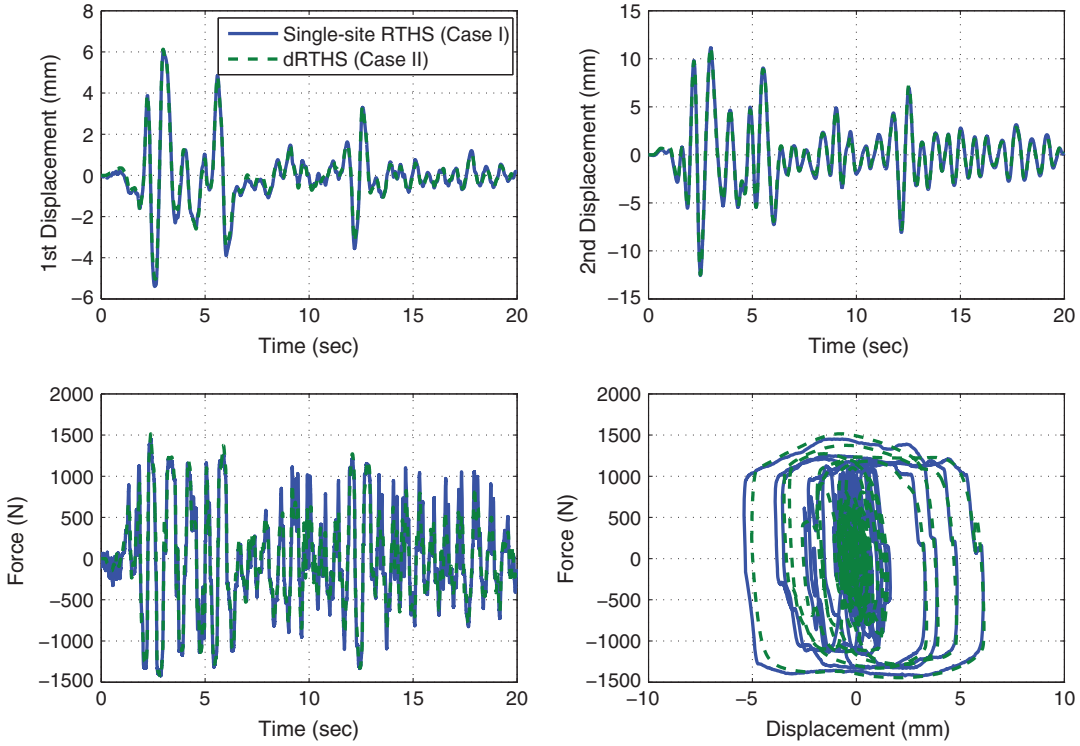

Fig. 17. (Color) Comparison of single-site and distributed test results—passive-on case

Distributed Real-Time Hybrid Simulation with Two Physical Substructures

A more sophisticated dRTHS is conducted in Case III, with two nonlinear physical substructures loaded by two actuators at geographically distributed sites, to verify the feasibility of the dRTHS framework and to investigate the performance of the MR damper control system. In Case III, the numerical substructure is located at UConn and the two MR dampers, as physical substructures, are tested in real time at Purdue and UConn concurrently. Cases include the passive-off system (0 V) and the passive-on system (3 V) with both MR dampers. Realistic modeling errors are included as the identified model from the Purdue MR damper is used for prediction models at both the remote and local sites. Pure numerical simulation of the two-story structural model with no MR dampers is conducted as a baseline uncontrolled case. A comparison of structural responses in uncontrolled, passive-off and passive-on modes is shown in Fig. 18. As observed in Fig. 18, the results demonstrate that stable dRTHS can be achieved for successful experimentation using this framework.

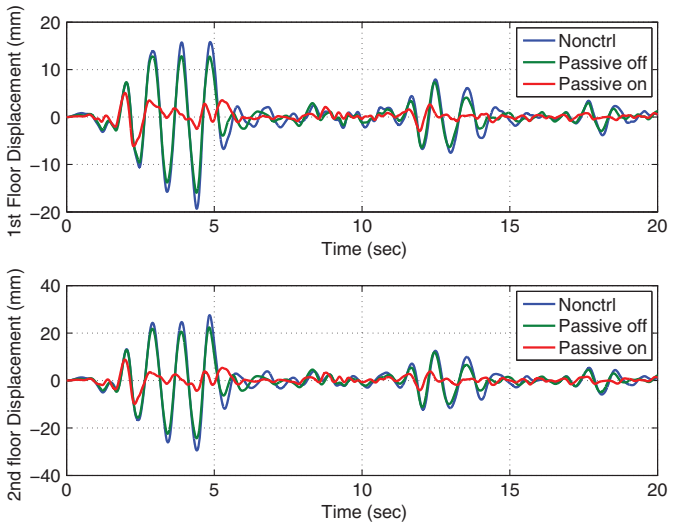

Fig. 18. (Color) Structural responses of each floor in Case III

Conclusions

The development of effective approaches for conducting distributed real-time hybrid simulations will broaden the range of experiments that can be addressed with RTHS, encouraging the coupling of laboratory capabilities to optimize the use of valuable institutional resources. Herein, we develop and experimentally verify a framework for conducting geographically distributed real-time hybrid simulations using a modified Smith predictor. Internet-induced time delays are effectively accommodated through the inclusion of the modified Smith predictor, whereas actuator dynamics and the associated time lags are compensated with actuator controllers. To evaluate the robustness of the architecture to network delays, a sensitivity study is first performed to consider a parametric analysis. Here, uncertainty is considered in the prediction models of the physical specimens used in modified Smith Predictor to accommodate network delay in experiment measurement. It is shown that small errors of lower than 5% can be achieved under real network conditions. The dRTHS framework is experimentally verified through a series of tests between Purdue and UConn, including tests with one nonlinear physical substructure and two nonlinear, distributed substructures. Comparisons between Case I (single-site RTHS) and Case II (dRTHS with one MR damper) demonstrate that dRTHS test results agree with those from single-site RTHS. In Case III, two physical substructures are included at Purdue and UConn. These results verify the approach and further demonstrate that dRTHS is achieved with the proposed method.

Acknowledgments

The authors gratefully acknowledge the partial support of this research by U.S. National Science Foundation under awards 1148255 and 1148215, the National Natural Science Foundation of China under awards 51261120377 and China Scholarship Council. The unique RTHS facilities in the Intelligent Infrastructure Systems Lab was developed through NSF CNS 1028668 and with support from Purdue University's School of Mechanical Engineering.

References

Campbell, S., and Stojadinovic, B. (1998). "A system for simultaneous pseudodynamic testing of multiple substructures." *Proc., 6th U.S. National Conf. on Earthquake Engineering*, Earthquake Engineering Research Institute, Seattle.

Carrion, J., and Spencer, B. F. (2007). "Model-based strategies for real-time hybrid testing." *Tech. Rep. NSEL-006*, Univ. of Illinois at Urbana-Champaign, Champaign, IL.

Dimig, J., Shield, C., French, C., Bailey, F., and Clark, A. (1999). "Effective force testing: A method of seismic simulation for structural testing." *J. Struct. Eng.*, 10.1061/(ASCE)0733-9445(1999)125:9(1028), 1028–1037.

Du, F., and Du, W. (2009). "A novel Smith predictor for wireless networked control systems with uncertainty." *ESIAT 2009, Int. Conf. on Environmental Science and Information Application Technology*, IEEE, New York.

Elnashai, A., Spencer, B., Kim, S. J., Holub, C., and Kwon, O. (2008). "Hybrid distributed simulation of a bridge-foundation-soil interaction system." *4th Int. Conf. on Bridge Maintenance, Safety, and Management*, CRC Press, Netherlands.

Friedman, A. J., et al. (2014). "Large-scale real-time hybrid simulation for evaluation of advanced damping system performance." *J. Struct. Eng.*, 141(6), 10.1061/(ASCE)ST.1943-541X.0001093, 04014150.

Gao, X. (2012). "Development of a robust framework for real-time hybrid simulation: From dynamical system, motion control to experimental error verification." Ph.D. dissertation, Schools of Civil Engineering and Mechanical Engineering, Purdue Univ., West Lafayette, IN.

Gao, X., Castaneda, N., and Dyke, S. (2013). "Experimental validation of a generalized procedure for MDOF real-time hybrid simulation." *J. Eng. Mech.*, 10.1061/(ASCE)EM.1943-7889.0000696, 04013006.

Horiuchi, T., Inoue, M., Konno, T., and Namita, Y. (1999). "Real-time hybrid experimental system with actuator delay compensation and its application to a piping system with energy absorber." *Earthquake Eng. Struct. Dyn.*, 28(10), 1121–1141.

Kim, S., Christenson, R., Phillips, B., and Spencer, B. (2012). "Geographically distributed real-time hybrid simulation of MR dampers for seismic hazard mitigation." *20th Analysis and Computation Specialty Conf.*, ASCE, Reston, VA.

lsqcurvefit [Computer software]. MathWorks, Natick, MA.

Maghareh, A., Dyke, S. J., Prakash, A., and Bunting, G. B. (2014a). "Establishing a predictive performance indicator for real-time hybrid simulation." *Earthquake Eng. Struct. Dyn.*, 43(15), 2299–2318.

Maghareh, A., Dyke, S. J., Prakash, A., and Rhoads, J. (2014b). "Establishing a stability switch criterion for effective implementation of real-time hybrid simulation." *Smart Struct. Syst.*, 14(6), 1221–1245.

Magonette, G., and Negro, P. (1998). "Verification of the pseudodynamic test method." *Eur. Earthquake Eng.*, 12(1), 40–50.

Mahin, S. A., Shing, P. B., Thewalt, C. R., and Hanson, R. D. (1989). "Pseudodynamic test method—Current status and future direction." *J. Struct. Eng.*, 10.1061/(ASCE)0733-9445(1989)115:8(2113), 2113–2128.

MATLAB [Computer Software]. MathWorks, Natick, MA.

Mosqueda, G., Stojadinovic, B., and Mahin, S. A. (2004). "Geographically distributed continuous hybrid simulation." *13th World Conf. on Earthquake Engineering*, International Association for Earthquake Engineering, Vancouver, BC, Canada.

Nakashima, M. (2001). "Development, potential, and limitation of real-time on-line (pseudo-dynamic) testing." *Math. Phys. Eng. Sci.*, 359(1786), 1851–1867.

Nakashima, M., and Masaoka, N. (1999). "Real-time on-line test for MDOF systems." *Earthquake Eng. Struct. Dyn.*, 28(4), 393–420.

Ojaghi, M., Williams, M. S., Dietz, M. S., Blakeborough, A., and Lamata Martínez, I. (2014). "Real-time distributed hybrid testing: Coupling geographically distributed scientific equipment across the Internet to extend seismic testing capabilities." *Earthquake Eng. Struct. Dyn.*, 43(7), 1023–1043.

OpenSees version 2.5.0 [Computer software]. Univ. of California, Berkeley, CA.

Ou, G., Ozdagli, A. I., Dyke, S. J., and Wu, B. (2015). "Robust integrated actuator control: Experimental verification and real-time hybrid-simulation implementation." *Earthquake Eng. Struct. Dyn.*, 44(3), 441–460.

Shing, P., Wei, Z., Jung, R. Y., and Staffer, E. (2004). "NEES fast hybrid test system at the University of Colorado." *Proc., 13th World Conf. on Earthquake Engineering*, International Association for Earthquake Engineering, Vancouver, BC, Canada.

Simulink Coder [Computer software]. MathWorks, Natick, MA.

Smith, O. J. (1959). "A controller to overcome dead time." *ISA J.*, 6(2), 28–33.

Spencer, B. F., Finholt, T., Foster, I., and Kesselman, C. (2004). "Neesgrid: A distributed collaboratory for advanced earthquake engineering experimentation and simulation." *Proc., 13th World Conf. on Earthquake Engineering*, International Association for Earthquake Engineering, Vancouver, BC, Canada.

Takahashi, Y., and Fenves, G. L. (2006). "Software framework for distributed experimental-computational simulation of structural systems." *Earthquake Eng. Struct. Dyn.*, 35(3), 267–291.

Takanashi, K., Udagawa, K., Seki, M., Okada, T., and Tanaka, H. (1975). "Non-linear earthquake response analysis of structures by a computer-actuator on-line system. Part 1: Detail of the system." *Trans. Archit. Inst. Jpn.*, 229, 77–83.

Tsai, K. C., Yeh, C. C., Yang, Y. C., Wang, K. J., and Chen, P. C. (2003). "Seismic hazard mitigation: Internet-based hybrid testing framework and examples." *Int. Colloquium on Natural Hazard Mitigation: Methods and Applications*, Université Pierre et Marie CURIE, Paris.

Watanabe, E., Yun, C. B., Sugiura, K., Park, D. U., and Nagata, K. (2001). "On-line interactive testing between KAIST and Kyoto University." *Proc., 14th KKNN Symp. on Civil Engineering*, KKNN Symposium, Kyoto, Japan.

xPC Target [Computer Software]. MathWorks, Natick, MA.